interaction of the more diffuse outer p shells with $V_{q,\infty}$. Significant contributions to γ_∞ arise from the charge density of these shells in regions which, for a typical environment, would be several layers of near neighboring nuclei out from the parent nucleus. $V_{q,\infty}$ is clearly inappropriate to such a region, as is the free ion function itself. The remedy does not lie in estimating V_q and evaluating an antishielding factor with it alone, for one must account for repercussions from other terms in the crystal potential,[16] and for interionic exchange, overlap and, on occasion, covalent and/or conduction electron effects from the environment. At the minimum one would be involved with the as yet incompletely understood matter of crystal field effects. We should note that an analytic uhf (and if need be many-centered) approach would be particularly adept for coping with the above complications.

We believe the Br^- and I^- γ_∞ values to appreciably overestimate the antishielding appropriate to experiment, though very likely less severely than is the case for Cl^-. The overestimate could easily be a factor of two for these ions.

Of greater interest to us is the case of rare-earth antishielding. One would like to think, from experience with positive ions such as Cu^+, that a γ_∞ of -80 is appropriate to experiment. Such a value is in good agreement with current Mössbauer effect estimates.[2] (Actually, any value between -30 and -150 would not be in serious disagreement with experiment.) Whether $\gamma_\infty \approx -80$ or not, external-field antishielding in rare-earth ions appears to be substantial, making the lattice electric-field gradient an experimentally significant quantity (see II).

ACKNOWLEDGMENTS

We are grateful to Dr. R. M. Sternheimer for conversations and for allowing us to quote his preliminary results. We are indebted to Mrs. Anna Hansen of the U. S. Army Materials Research Agency for help with some of the computations.

PHYSICAL REVIEW VOLUME 135, NUMBER 5A 31 AUGUST 1964

Atomic Absorption Cross Section of Sodium Vapor Between 2400 and 1000 Å

R. D. HUDSON
Aerospace Corporation, El Segundo, California
(Received 8 April 1964)

The continuous atomic absorption cross section of sodium vapor has been measured using photoelectric techniques from the $3s\,^2S \rightarrow np\,^2P^0$ series limit at 2412.6 Å, down to 1000 Å. The bandwidth of the monochromator was 1 Å, and values of the cross section were obtained at about 2-Å intervals. The best value for the atomic absorption cross section at the series limit was 0.130 ± 0.018 Mb. A zero minimum was observed at 1950 Å, in agreement with theoretical predictions but conflicting with previous experimental results. The reasons for this conflict are discussed, and a description is given of the experimental procedures adopted.

I. INTRODUCTION

THE alkali metals form one group in which theory and experiment can be compared most favorably. Ditchburn and Öpik[1] have recently summarized the results obtained for the continuous absorption cross section of these metals and conclude that the agreement between theory and experiment is good for photon energies up to about 2 eV above the ionization limit. The agreement is not good at higher energies for, with the exception of lithium, the balancing of the positive and the negative contributions to the transition integral is so close that unless the initial wave functions chosen are exact, accurate calculations are almost impossible.

It would not be fair, however, to dismiss any disagreement that now exists between theory and experiment as being due only to the theory. It was therefore decided to measure the continuous absorption cross section of the alkali metals using improved techniques. This paper is an account of the results obtained for sodium.

II. DETERMINATION OF THE ATOMIC ABSORPTION CROSS SECTION OF METALLIC VAPORS

A. Absorption Cross Section

The absorption cross section $\sigma(\lambda)$ of a single species in the gaseous or vapor state is defined as follows:

$$\ln\frac{I_0(\lambda)}{I(\lambda)} = N\sigma(\lambda)\frac{273}{T}\frac{p}{760}L, \tag{1}$$

where $I_0(\lambda)$ and $I(\lambda)$ are, respectively, the intensity incident on and transmitted through the column of vapor or gas, of length L, at a pressure of p mm Hg and at an absolute temperature T, and where N is Loschmidt's number.

[1] R. W. Ditchburn and V. Öpik, in *Atomic and Molecular Processes*, edited by D. R. Bates (Academic Press Inc., New York, 1962).

In order to obtain accurate values of $\sigma(\lambda)$, the following conditions must be satisfied: (1) The vapor must be free from impurities. (2) The ratio of I_0 to I must be measured accurately. (3) The path length L and the pressure p of the gas or vapor must be well defined. If this cannot be done, then $\int_0^L p dL$ must be well defined.

B. Path Length and Pressure Determination for Metallic Vapors

The alkali metal vapors are all corrosive and thus windows cannot be used to confine the vapor, as they would be rapidly attacked at the temperatures needed to obtain vapor pressures suitable for absorption spectroscopy. Early experimenters placed the active metal at the center of a long steel tube and prevented the metal vapor from diffusing rapidly to the cool ends of the tube by filling it with an inert gas at a pressure of several atmospheres. This method suffers from two serious disadvantages: (1) the pressure of the vapor at any point in the tube cannot be defined, and (2) the high pressure of the inert gas can change the absorption cross section one is trying to measure.

The technique developed by Ditchburn, Tunstead, and Yates[2] to overcome this problem was used in the present experiment. The absorption tube used for sodium vapor is shown schematically in Fig. 1. The metal is placed in boats near the ends of the absorption tube, and the whole system is filled with an inert gas at a few mm Hg. The absorption tube is then raised to the desired temperature. The vapor from the boats will now diffuse slowly through the inert gas but, due to the metal plugs between the boats and the end of the furnace, the rate of diffusion to the cold parts of the tube is extremely small. Thus in equilibrium one has a column of vapor between the boats at a pressure given by the vapor pressure of the metal above the boats. The $\int_0^L p dL$ for the region from the boats to the condensation point of the vapor can be calculated using diffusion theory. It is estimated that in the present experiment the over-all $\int_0^L p dL$ could be obtained to within $\pm 3\%$.

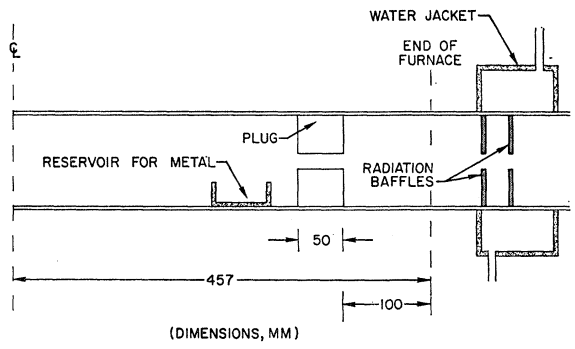

FIG. 1. Schematic diagram of absorption tube.

[2] R. W. Ditchburn, J. Tunstead, and J. G. Yates, Proc. Roy. Soc. (London) A181, 386 (1943).

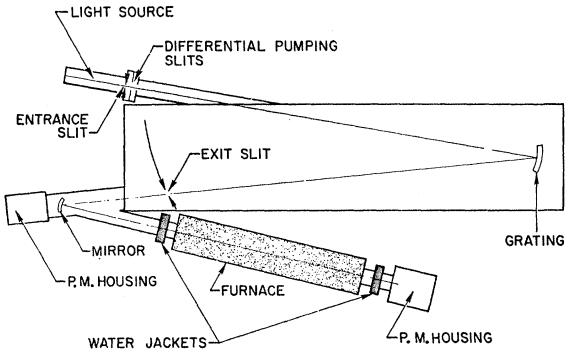

FIG. 2. The 2-m monochromator and associated equipment.

The pressure of the inert gas does not need to be more than 2 mm Hg above the vapor pressure of the metal. The required metal vapor pressure is only a few mm Hg, and the pressure effects due to the inert gas, therefore, become insignificant. As an added precaution, helium is used as the filling gas.

C. Molecular Absorption

The vapors of the alkali metals at a few mm Hg contain quite a high percentage of the diatomic molecule (from 1 to 10%). Thus Eq. (1) should strictly be written as follows:

$$\ln\frac{I_0(\lambda)}{I(\lambda)}=C_a\sigma_a(\lambda)L_a+C_m\sigma_m(\lambda)L_m, \qquad (2)$$

where C_a and C_m are the concentrations of the atomic and molecular species, respectively. In the case of sodium, σ_m was found to be an order of magnitude higher than σ_a, and thus, in order to obtain accurate values of σ_a, some way had to be found to separate the absorption of the two species. The exact method of separation will be discussed in Sec. V.

III. EXPERIMENTAL APPARATUS

The apparatus used in the experiment is shown in Fig. 2 and is described in the following paragraphs.

A. Light Source

Two different types of light sources were used: a hydrogen-discharge source and a condensed-discharge argon continuum source. The former produces a many-lined spectrum between 1000 and 1650 Å and a continuum between 1650 and 3700 Å. The condensed-discharge argon continuum source, which has been described previously by Cook and Metzger,[3] gives a continuum that extends from 1050 to 1600 Å. Both of these light sources were separated from the body of the spectrograph by a differential pumping slit.

[3] P. H. Metzger and G. R. Cook, J. Quant. Spectry. Radiative Transfer 4, 107 (1964).

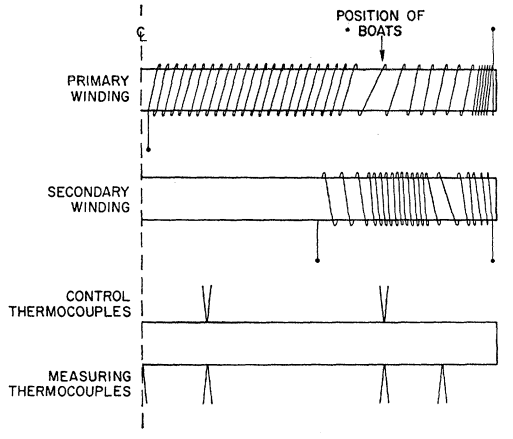

FIG. 3. Schematic diagram of windings and placement of thermocouples along furnace tubes (right-hand half only shown).

B. Monochromator

The monochromator was a 2.2-m normal-incidence combination spectrograph and scanning monochromator (Eagle Mount) manufactured by the McPherson Instruments Company. The grating was a Bausch and Lomb replica with 600 lines/mm blazed in first order at 1500 Å. With this grating, the spectrograph had an inverse dispersion of 7.5 Å/mm in first order. The slit widths were set to give a bandwidth of about 1 Å.

C. Mirror Chamber

The beam of light from the monochromator exit slit was reflected from a concave mirror, as shown in Fig. 2, and brought to a focus on a sodium salycilate screen in front of a photomultiplier at the far end of the absorption tube. The principal purpose of the mirror was to convert the diverging beam from the exit slit to a converging beam through the absorption tube. This meant that the radiation baffles in front of the photomultiplier could be made with narrow openings, limiting the amount of infrared radiation from the hot furnace tube that could reach the photomultiplier. The mirror had a hole bored in its center so that the incident intensity from the exit slit could be monitored by a photomultiplier assembly placed behind the mirror.

For the spectral region from 1500 to 3700 Å, the mirror was coated with aluminum, which has a high reflectivity in this region. Aluminum could not be used between 1000 and 1500 Å, however, as its reflectivity in this region dropped rapidly when the temperature of the furnace tube was raised to 500°C [e.g., the reflectivity at Lyman-α (1215 Å) dropped from 10% to 1% in about 60 min]. This is probably due to the formation of an additional oxide coating by the infrared radiation from the tube. Thus, for the region from 900 to 1500 Å, a gold coating was used on the mirror, for, although the reflectivity is also only 10% at Lyman-α, it was unaffected by the radiation from the furnace tube.

D. Absorption Chamber

A schematic diagram of the absorption tube with some of the appropriate dimensions is shown in Fig. 1. The absorption tube, the metal reservoirs, and the plugs were manufactured from type-304 stainless steel and were all thoroughly degreased before use. The water jackets were placed 2 in. from either end of the furnace to prevent the conduction of heat to the rest of the apparatus and also to condense the last remains of metallic vapor. The radiation baffles were placed at the same position as the water jackets to keep the baffles cool. The plugs, metal reservoirs, and baffles were joined together with support rods, and the entire unit was made to slide in or out of the absorption tube.

The furnace consisted of two sets of windings of Nichrome wire on a cylindrical ceramic former, insulated from one another by a layer of asbestos rope. The outer winding was then lagged with several more layers of asbestos rope to prevent excessive heat losses. Details of the furnace windings are shown in Fig. 3. It can be seen that the temperature at the middle of the furnace tube will be controlled by the primary winding, while that at the metal boats will be controlled by the secondary winding.

The temperature of the absorption tube was controlled by four temperature controllers, actuated by Chromel-Alumel thermocouples placed as shown in Fig. 3. The temperature was measured at these four points and at three others (see Fig. 3) with independent Chromel-Alumel thermocouples through a multipoint recorder. The thermocouple recorder combination was calibrated against a standardized platinum versus platinum +10% rhodium thermocouple. Using these procedures, it is estimated that the temperature of the furnace could be measured to within ±2°C between 400 and 500°C. The temperature controllers could not be set to give an ultimate temperature as accurately as this and, in practice, the settings were adjusted until the temperatures, as measured by the thermocouple-recorder combination, were the same down the entire length of the absorption tube. The over-all temperature variation at 500°C over a period of some 60 min was never more than ±2°C, corresponding to a pressure variation in the vapor of less than ±5%.

E. Detector Arrangement

A problem in trying to measure the absorption coefficient of metallic vapors with a monochromator is the infrared radiation emitted by the furnace tube. This is expecially true if one wishes to investigate the region below 1100 Å, as solar blind photomultipliers are limited by their window material, and open photomultipliers cannot be used at the helium pressures employed in the absorption tube. Consequently, it was decided to use a sodium salycilate covered window, behind which was placed an E.M.I. No. 6255S photomultiplier tube. The photomultiplier principally affected by the radiation

from the furnace tube was that at the end of the absorption tube. The problem was alleviated (as was discussed in Sec. IIIC) by using the mirror and baffles but it was also found necessary to place a Kodak Wratten filter No. 47B between the salycilate screen and the photomultiplier. This filter has a pass band of about 100 Å centered at 3800 Å, the wavelength at which the fluorescence from sodium salycilate is a maximum.

The object of the photomultiplier behind the mirror was to monitor the incident intensity, and that of the photomultiplier at the end of the furnace tube to measure $I_0(\lambda)$ before the experiment and $I^1(\lambda)$ during the experiment. Let the corresponding values of the mirror photomultiplier be called $A_0(\lambda)$ and $A_0{}^1(\lambda)$. If the ratio $[I_0(\lambda)]/[A_0(\lambda)]=\beta(\lambda)$ can be assumed to be constant throughout the experiment, then the value of the incident radiation on the vapor during the experiment, $I_0{}^1(\lambda)$, will be given by $I_0{}^1(\lambda)=A_0{}^1(\lambda)\beta(\lambda)$. The advantage of using the two photomultipliers was that any change in $I_0(\lambda)$ during the experiment was automatically compensated for.

Tests were carried out before each experiment with the inner assembly in the absorption tube but with no sodium in the boats to check that $\beta(\lambda)$ was a constant over the temperature range to be used.

IV. EXPERIMENTAL PROCEDURE

Solid lumps of sodium metal with a purity of 99.99% were used in the experiments described in this paper. The freshly cut metal was washed in ethyl alcohol to remove surface impurities and loaded into the metal reservoirs. The inner assembly was then pushed into the absorption tube and the whole system was pumped down to a pressure of 10^{-5} mm Hg, while the temperature of the absorption tube was raised to 150°C and maintained at this level for several hours. This temperature was high enough to melt the sodium metal and hence drive off any organic impurities trapped in the matrix of the metal, but not so high that too much metal was lost from the boats. When outgassing had ceased, the tube was filled with helium at a pressure above 10 mm Hg, and the cell temperature was raised to 500°C (corresponding to a sodium vapor pressure of 4 mm Hg). The absorption tube was kept at this temperature for about two hours, cooled rapidly to 150°C, and pumped down to 10^{-5} mm Hg. This procedure was found to remove all of the organic impurities.

At the start of an experimental run the tube was filled with helium, at a suitable pressure for the experiment, and raised to a temperature of 300°C, where the vapor pressure of the sodium was still low enough to produce negligible absorption. The emission spectrum of the light source over the spectral range being investigated was then scanned with the monochromator with both $I_0(\lambda)$ and $A_0(\lambda)$ being recorded simultaneously, as described in Sec. IIIE. This procedure was repeated twice. The absorption tube was then raised to the working temperature, and $I^1(\lambda)$ and $A_0{}^1(\lambda)$ were recorded twice. The temperature was then changed by 10°C intervals and this procedure repeated. At the end of a set of absorption runs, the temperature of the absorption tube was lowered to 300°C, and traces of $I_0(\lambda)$ and $A_0(\lambda)$ versus wavelength were again recorded. The sets of runs at 300°C were used to obtain an average value of $\beta(\lambda)$ (see Sec. IIIE). The deviation from the mean of $\beta(\lambda)$ was always less than 2%, for if it became greater than this, the set of runs was discarded.

The recorder traces were converted to a digital form on an $X-Y$ chart reader, and a digital computer then converted the readings of $I_0(\lambda)$, $A_0(\lambda)$, $I^1(\lambda)$, and $A_0{}^1(\lambda)$ to the ratio $[I_0{}^1(\lambda)]/[I^1(\lambda)]$ at wavelength intervals of 2 Å.

TABLE I. Comparison of recent compilations of thermochemical data for atomic sodium vapor.

Paper	Vapor pressure, mm Hg 600°K	700°K	800°K	900°K
JANAF (Ref. 4)	0.040	0.732	6.41	34.1
Hultgren *et al.* (Ref. 5)	0.039	0.740	6.54	35.6
Honig (Ref. 6)	0.039	0.708	6.29	34.1
Nesmeyanov (Ref. 7)	0.034	0.750	6.61	35.0

V. SEPARATION OF THE ATOMIC AND MOLECULAR ABSORPTION CROSS SECTIONS

In order to separate the atomic and molecular cross sections, Eq. (2) must be solved. The term $\ln[I_0(\lambda)]/[I(\lambda)]$ is obtained as described in the previous section, but the evaluation of the constants L_a, L_m, $C_a(\lambda)$, and $C_m(\lambda)$ depends uniquely on a knowledge of the variation of the vapor pressures of the two constituents with temperature.

The variation of the vapor pressure of atomic sodium with temperature has been reviewed within the past year in four papers,[4–7] and the values over the temperature range of the present experiment are given in Table I. The agreement between the sets is within ±3%. The variation of the vapor pressure of molecular sodium has been reviewed in two of these four papers,

TABLE II. Comparison of recent compilations of thermochemical data for molecular sodium vapor.

Paper	Vapor pressure, mm Hg 600°K	700°K	800°K	900°K
JANAF (Ref. 4)	0.00109	0.0385	0.533	3.99
Nesmeyanov (Ref. 7)	0.00048	0.0193	0.296	2.36

[4] JANAF Thermochemical Tables (The Dow Chemical Company, Midland, Michigan, 1962).

[5] R. Hultgren, R. L. Orr, P. D. Anderson, and K. K. Kelley, *Selected Values of Thermodynamic Properties of Metals and Alloys* (John Wiley & Sons, Inc., New York, 1963).

[6] R. E. Honig, RCA Rev. **23**, 567 (1962).

[7] A. N. Nesmeyanov, in *Vapor Pressure of the Chemical Elements*, edited by Robert Gary (Elsevier Publishing Co., Inc., New York, 1963).

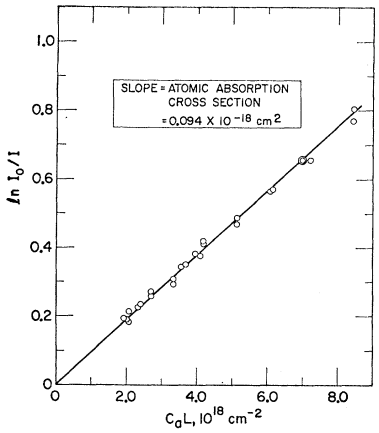

FIG. 4. ln I_0/I versus C_aL at 1500Å.

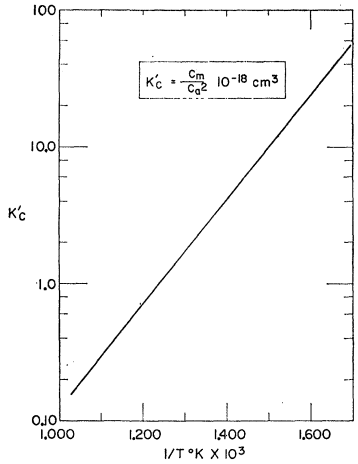

FIG. 6. K_c' versus $1/T$°K (from JANAF data).

and these results are given in Table II. The results quoted by Nesmeyanov are taken from calculations made by Gordon[8] in 1936, while the JANAF results are recent calculations (1962) carried out by the thermal laboratory of the Dow Chemical Company. The JANAF results are based on more accurate spectroscopic constants and should therefore be more dependable. The final vapor-pressure formulae chosen for both the atomic and the molecular species were those given in the JANAF tables.

If at any wavelength $\sigma_a(\lambda)$ or $\sigma_m(\lambda)$ is zero, then Eq. (2) reduces to

$$\ln I_0/I = C\sigma(\lambda)L,$$

and a plot of $\ln I_0/I$ versus CL will give a straight line running through the origin. Figure 4 shows such a plot for results at 1500 Å, where σ_m is zero, while Fig. 5 shows plots for results at three wavelengths greater than that corresponding to the series limit, i.e., where σ_a is zero. The straight lines obtained indicate that the vapor-pressure data used in this paper are reasonably accurate.

The method of separation used is different from that adopted by Ditchburn, Jutsum, and Marr.[9] By the law of mass action

$$C_m/C_a^2 = K_c'(T),$$

where K_c' is the equilibrium constant. Thus, Eq. (2) may be rewritten as follows:

$$\ln[I_0(\lambda)]/[I(\lambda)] = C_a\sigma_a(\lambda)L + C_a^2K_c'\sigma_m(\lambda)L \quad (3)$$

or

$$\frac{\ln[I_0(\lambda)]/[I(\lambda)]}{C_aL} = \sigma_a(\lambda) + C_aK_c'\sigma_m(\lambda). \quad (4)$$

Ditchburn, Jutsum, and Marr solved for $\sigma_a(\lambda)$ by assuming that K_c' would be a constant over the temperature range used in their experiment. Equation (4) then becomes the equation of a straight line, the intercept of which is $\sigma_a(\lambda)$. However, the JANAF tables[4] do not support this assumption, and as can be seen from Fig. 6, K_c' varies rapidly with temperature. It can be shown that the method of separation adopted by Ditchburn *et al.*, will always give a finite value to $\sigma_a(\lambda)$, if $\sigma_m(\lambda) \neq 0$, even if $\sigma_a(\lambda)$ is in fact zero.

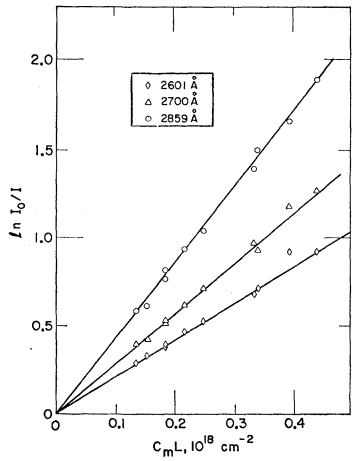

FIG. 5. ln I_0/I versus C_mL at three wavelengths longer than the series limit.

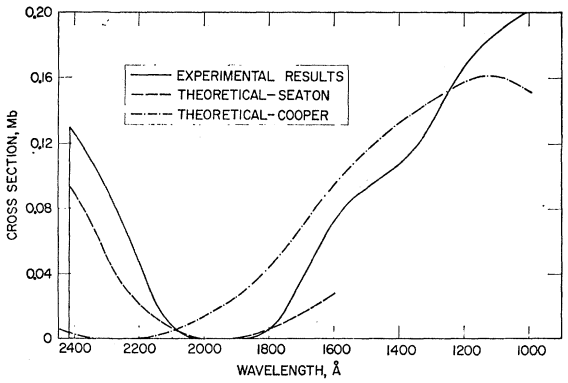

FIG. 7. Atomic absorption cross section versus wavelength.

[8] A. R. Gordon, J. Chem. Phys. 4, 100 (1936).

[9] R. W. Ditchburn, P. J. Jutsum, and G. V. Marr, Proc. Roy. Soc. (London) **A219**, 89 (1953).

The final values of $\sigma_a(\lambda)$ and $\sigma_m(\lambda)$ adopted were obtained from a least-squares analysis of the results taken at more than 20 different temperatures.

VI. RESULTS

A plot of the atomic absorption cross section versus wavelength from the series limit to 1000 Å is shown as the continuous line in Fig. 7, and a plot of the molecular cross section over the same spectral range is shown in Fig. 8.

The standard deviation obtained for the atomic cross section from the least-squares program was 10% at the series limit, giving a standard error of the mean of 2%. The systematic error arising from the temperature calibration is 4% and that from the estimation of the path length is 3%, giving a total error of ±9%. There is also an inherent error from the vapor-pressure formula assumed, which is compounded by the dependence of the calculated atomic absorption cross section on both the atomic and molecular concentrations. This error is not easy to assess, but is believed to be of the order of ±5%. The best value obtained for the atomic absorption cross section at the series limit of the $3s\,^2S \rightarrow np\,^2P^0$ series was 0.130±0.018 Mb (1 Mb$=10^{-18}$ cm^2). This result agrees within experimental error with that of 0.116±0.013 Mb obtained by Ditchburn, Jutsum, and Marr.[9]

As one moves towards shorter wavelengths, the absorption cross section drops rapidly, and at 1950 Å there is an apparent zero minimum. It seems probable that the zero minimum is real, but considerations of the experimental error place an upper limit to the atomic absorption cross section at this point of 0.003 Mb. Below 1950 Å the cross section rises rapidly, and at 1050 Å it has a value of 0.195±0.027 Mb. The general indication is that the cross section continues to rise at least as far as 900 Å.

The detection of a zero minimum at 1950 Å is in direct conflict with the findings of Ditchburn, Jutsum, and Marr, who detected a finite minimum at the same wavelength. As has been discussed in Sec. V, their nonzero minimum is thought to be the result of using incorrect thermochemical data.

VII. DISCUSSION OF THE RESULTS

Figure 7 also shows two theoretical predictions of the variation of the atomic absorption cross section with wavelength. The results obtained by Seaton[10] were calculated using Hartree-Fock wave functions with the dipole length formulation. Those of Cooper[11] were calculated using a simplified one-electron model based on the effective central potential obtained from Hartree-Fock ground-state orbitals; they are to be considered a good first approximation. Another theoretical curve obtained by Burgess and Seaton[12] has not been included in Fig. 7 for the sake of clarity. This calculation was performed using the quantum-defect method[13] and yields a cross section at the series limit of 0.18 Mb with a zero minimum near 1800 Å.

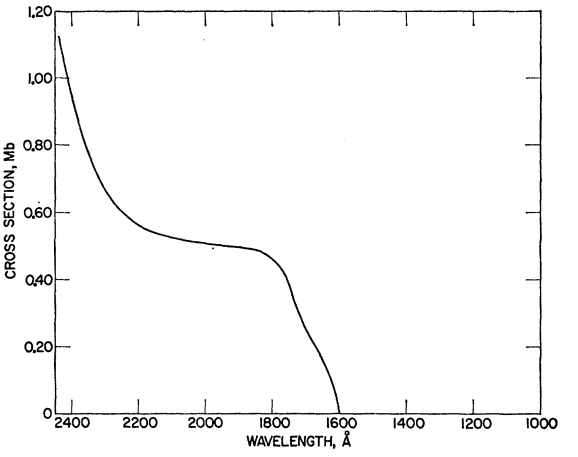

FIG. 8. Molecular absorption cross section versus wavelength.

The one common feature of all of these theoretical predictions is a zero minimum near the series limit due to the complete cancellation of the positive and negative integrands. Of the theoretical results presented, only those of Seaton[10] seem to be in agreement with the present experimental results as to the wavelength corresponding to this minimum.

It may be argued that, apart from the minimum, the agreement between theory and experiment is still not good; however, in view of the fact that both Seaton and Cooper used only approximate wave functions, the agreement is remarkably good, for both theoretical curves predict the gross features (magnitude and spectral shape) of the cross section.

ACKNOWLEDGMENTS

My sincere thanks are due to Dr. R. A. Becker for his help and encouragement in this work, and to R. Marcoe for his able technical assistance. I should also like to acknowledge many helpful discussions with Dr. G. R. Cook and Miss V. L. Carter.

[10] M. J. Seaton, Proc. Roy. Soc. (London) **A208**, 418 (1951).
[11] J. W. Cooper, Phys. Rev. **128**, 681 (1962).
[12] A. Burgess and M. J. Seaton, Monthly Notices Roy. Astron. Soc. **120**, 121 (1960).
[13] M. J. Seaton, Monthly Notices Roy. Astron. Soc. **118**, 504 (1958).